Radial volumetric imaging breath-hold examination (VIBE) with k-space weighted image contrast (KWIC) for dynamic gadoxetic acid (Gd-EOB-DTPA)-enhanced MRI of the liver: advantages over Cartesian VIBE in the arterial phase

Yasunari Fujinaga · Ayumi Ohya · Hirokazu Tokoro · Akira Yamada · Kazuhiko Ueda ·
Hitoshi Ueda · Yoshihiro Kitou · Yasuo Adachi · Aya Shiobara · Naomichi Tamaru ·
Marcel D. Nickel · Katsuya Maruyama · Masumi Kadoya

Abstract

Objectives To compare radial volumetric imaging breath-hold examination with k-space weighted image contrast reconstruction (r-VIBE-KWIC) to Cartesian VIBE (c-VIBE) in arterial phase dynamic gadoxetic acid (Gd-EOB-DTPA)-enhanced magnetic resonance imaging (DCE-MRI) of the liver.
Methods We reviewed 53 consecutive DCE-MRI studies performed on a 3-T unit using c-VIBE and 53 consecutive cases performed using r-VIBE-KWIC with full-frame image subset (r-VIBE$_{full}$) and sub-frame image subsets (r-VIBE$_{sub}$; temporal resolution, 2.5–3 s). All arterial phase images were scored by two readers on: (1) contrast-enhancement ratio (CER) in the abdominal aorta; (2) scan timing; (3) artefacts; (4) visualisation of the common, right, and left hepatic arteries.
Results Mean abdominal aortic CERs for c-VIBE, r-VIBE$_{full}$, and r-VIBE$_{sub}$ were 3.2, 4.3 and 6.5, respectively. There were significant differences between each group ($P<0.0001$). The mean score for c-VIBE was significantly lower than that for r-VIBE$_{full}$ and r-VIBE$_{sub}$ in all factors except for visualisation of the common hepatic artery ($P<0.05$). The mean score of all factors except for scan timing for r-VIBE$_{sub}$ was not significantly different from that for r-VIBE$_{full}$.
Conclusions Radial VIBE-KWIC provides higher image quality than c-VIBE, and r-VIBE$_{sub}$ features high temporal resolution without image degradation in arterial phase DCE-MRI.
Key Points
• *Radial VIBE-KWIC minimised artefact and produced high-quality and high-temporal-resolution images.*
• *Maximum abdominal aortic enhancement was observed on sub-frame images of r-VIBE-KWIC.*
• *Using r-VIBE-KWIC, optimal arterial phase images were obtained in over 90 %.*
• *Using r-VIBE-KWIC, visualisation of the hepatic arteries was improved.*
• *A two-reader study revealed r-VIBE-KWIC's advantages over Cartesian VIBE.*

Y. Fujinaga (✉) · A. Ohya · H. Tokoro · A. Yamada · K. Ueda ·
M. Kadoya
Department of Radiology, Shinshu University School of Medicine,
3-1-1 Asahi, Matsumoto 390-8621, Japan
e-mail: fujinaga@shinshu-u.ac.jp

H. Ueda · Y. Kitou · Y. Adachi · A. Shiobara · N. Tamaru
Radiology Division of Shinshu University Hospital, Matsumoto,
Japan

M. D. Nickel
Siemens AG Healthcare Sector, H IM MR PI TIO Oncology,
Erlangen, Germany

K. Maruyama
Imaging & Therapy Systems Division, Siemens Japan. K. K.,
Shinagawa, Tokyo, Japan

Abbreviations

VIBE	Volumetric imaging breath-hold examination
KWIC	k-space weighted image contrast reconstruction
DCE-MRI	Dynamic contrast-enhanced magnetic resonance imaging
CER	Contrast-enhancement ratio

Introduction

Dynamic contrast-enhanced magnetic resonance imaging (DCE-MRI) is recognised as a useful method for detecting and characterising liver lesions. Assessment of lesion vascularity in the arterial phase is important for the detection of hypervascular neoplasms such as hepatocellular carcinoma. Gadoxetic acid (Gd-EOB-DTPA, Bayer Schering Pharma, Berlin, Germany), a hepatocyte-specific contrast agent [1, 2], has been used worldwide for contrast-enhanced MRI of the liver. The hepatobiliary phase of Gd-EOB-DTPA-enhanced MRI definitely shows improved lesion detectability [3–6]. In addition, lesion vascularity can be assessed using dynamic contrast-enhanced MRI (DCE-MRI) using Gd-EOB-DTPA as a non-specific extracellular T1-shortening contrast agent during the arterial phase.

Gd-EOB-DTPA, however, has the major drawback of less arterial enhancement compared with another hepatocyte-specific contrast agent, gadobenate dimeglumine (Gd-BOPTA; MultiHance, Barco, Italy), as well as less enhancement than that seen with non-specific extracellular contrast agents such as gadopentetate dimeglumine (Gd-DTPA; Bayer Schering Pharma, Berlin, Germany) [7–9]. Because the recommended dose of Gd-EOB-DTPA is lower than that of Gd-BOPTA and the extracellular contrast agents, there are some other problems on arterial phase DCE-MR images. Sometimes they cannot be obtained at the optimal scan time because the window of peak enhancement with Gd-EOB-DTPA is narrower than that with Gd- DTPA, assuming the same rate of injection [10]. Second, truncation or Gibbs artefact (so-called 'ringing artefact') is sometimes obvious on arterial phase DCE-MR images using Gd-EOB-DTPA [11]. Some authors attribute this problem to steep signal changes during sampling of k-space [10, 12].

New imaging sequences are desirable to compensate for the shortcomings of DCE-MRI using Gd-EOB-DTPA. The radial volumetric imaging breath-hold examination (r-VIBE), which is a modified version of Cartesian (traditional) VIBE (c-VIBE), is a new three-dimensional (3D) gradient-echo sequence. The r-VIBE features several advantages over the c-VIBE sequence, including less motion sensitivity, absence of aliasing artefacts, and less degradation of the image quality due to undersampling [13, 14]. Furthermore, r-VIBE with k-space-weighted image contrast reconstruction (r-VIBE-KWIC) allows view sharing and obtains high-temporal-resolution sub-frame (time-resolved) images as well as a full-frame image. For these reasons, some authors have reported that free-breathing DCE-MRI using r-VIBE-KWIC is a useful technique for analysis of abdominal organ perfusion [15, 16]. Reports suggest that r-VIBE-KWIC has the potential to produce good quality and high-temporal-resolution (time-resolved) arterial phase images on DCE-MRI with Gd-EOB-DTPA. Brodsky et al. [17] reported another type of time-

resolved 3D radial sequence, in which the scan sampled k-space uniformly using half-echo radial sampling during interleaved sub-frames acquisition, with high temporal and spatial resolution resulting. The drawback of this technique is that the reconstruction takes 14 min per frame.

Precise evaluation of the haemodynamics of liver tumours allows improved diagnostic accuracy. Single-level dynamic computed tomography during hepatic arteriography (CTHA) features high spatial and temporal resolution, and is able to demonstrate detailed characteristics of hypervascular lesions such as hepatocellular carcinoma (HCC) [18] and focal nodular hyperplasia (FNH) [19], though it is a relatively invasive technique with the added drawback of radiation exposure compared with DCE-MRI. Recently, advances in multidetector-row CT (MDCT) with more than 64 channels have enabled precise evaluation of haemodynamics with high spatial and temporal resolution without the necessity of arterial injection, but still necessitating radiation exposure. DCE-MRI using r-VIBE-KWIC, which requires neither arterial injection nor radiation exposure, has the potential to provide high-quality images, useful not only in detection but also in characterisation of hypervascular hepatic lesions. The advantages of breath-hold arterial phase DCE-MRI using r-VIBE-KWIC have not been analysed in comparison with c-VIBE. In this preliminary study, we aimed to compare r-VIBE-KWIC with c-VIBE in arterial phase DCE-MRI of the liver.

Materials and methods

The study protocol was approved by our Institutional Review Board. Written informed consent was obtained from all participating patients before the MRI examinations.

Patients

We retrospectively reviewed the database on DCE-MRI in our hospital. Fifty-three consecutive patients (28 men and 25 women; mean age 66.2 years old) who underwent DCE-MRI for liver disease using c-VIBE between May 2008 and September 2008, and 53 consecutive patients (31 men and 22 women; mean age 66.9 years old) who underwent DCE-MRI using r-VIBE-KWIC between June 2012 and July 2012 were selected for this study. Two patients underwent both examinations. No patients had renal dysfunction. Detailed characteristics of the patients in the two groups are shown in Table 1. Forty patients in the c-VIBE group and 31 patients in the r-VIBE-KWIC group had chronic liver disease, including HCC. In chronic liver disease group, liver function was evaluated with the Child-Pugh classification system. Of 40 patients in c-VIBE group, 35 patients were classified as A, 5 patients as B. Of 31 patients in r-VIBE-KWIC group, 30 patients were classified as A, 1 patient as B. Development of collateral

Table 1 Characteristics of the patients in two groups

	c-VIBE	r-VIBE-KWIC	P value
Number of patients	53	53	
Age (mean years)	66.3	66.9	0.82 [a]
Males/females	28/25	31/22	0.70 [b]
Body weight (mean kg)	54.7	60.5	0.06 [a]
Patient background			
Chronic liver disease (including HCC)	40	31	0.10 [b]
Child-Pugh classification			0.22 [b]
Grade A	35	30	
Grade B	5	1	
Development of collateral veins			0.78 [b]
Present	9	8	
Absent	31	22	
Malignant tumours (except for HCC)	12	21	0.09 [b]
Digestive tract cancer	5	4	
Pancreatic cancer or Malignant NET	3	6	
Cholangiocarcinoma	2	3	
Breast cancer	2	1	
Bile duct cancer	0	3	
Gynaecological cancer	0	4	
Bile duct stone	1	1	1.00 [b]

c-VIBE Cartesian volumetric imaging breath-hold examination, r-VIBE-KWIC Radial volumetric imaging breath-hold examination with k-space weighted image contrast reconstruction; HCC hepatocellular carcinoma, NET neuroendocrine tumour

[a] P values were calculated by Mann–Whitney U test
[b] Calculated by Fisher's extract test

veins, which indicated portal hypertension, was seen in nine patients in c-VIBE group and eight patients in r-VIBE-KWIC group. Twelve patients in the c-VIBE group and 21 patients in the r-VIBE group had a malignant tumour other than HCC, and underwent liver MRI for survey of liver metastasis. One patient, each in the c-VIBE and r-VIBE-KWIC groups, had a history of bile duct stones. All patients without chronic liver disease had no liver dysfunction. There was no significant difference in age, gender, body weight, Child-Pugh classification, development of collateral veins and prevalence of diseases between the two groups.

MRI data acquisition

All MR images were obtained with a 3-T MR unit (Magnetom Trio; Siemens Medical Systems, Erlangen, Germany) using a standard body array coil and a spine matrix coil provided by the manufacturer. The sequence parameters of c-VIBE and r-VIBE-KWIC are shown in Table 2. We used generalised auto-calibrating partially parallel acquisition (GRAPPA) [20] with an acceleration factor of 2 to optimise the sequences in c-

Table 2 Scan parameters of the two sequences

	c-VIBE	r-VIBE-KWIC
Repetition time (ms)	3.5–4	2.51–3.5
Echo time (ms)	1.4	1.11–1.43
Flip angle (degree)	13–15	11–12
Matrix size	320×123–177	192×192
Section thickness (mm)	2.7–4	3–4.3
Field of view (mm)	400–420×210–289	260–340×260–340
Acquisition time (s)	18–24	20–24

c-VIBE Cartesian volumetric imaging breath-hold examination, r-VIBE-KWIC radial VIBE with k-space weighted image contrast

VIBE. Each parameter was adjusted to yield a breath-hold time of approximately 20 s.

Imaging protocol of DCE-MRI

In all patients, we used a standard dose of Gd-EOB-DTPA (0.025 mmol/kg body weight). After placing a 21-gauge catheter in the cubital vein, the contrast agent was injected at a rate of 2 ml/s followed by 40 ml of 0.9 % saline at the same rate. Precontrast and three-phase DCE-MR images were acquired. Arterial phase images were obtained using a bolus timing technique in the c-VIBE group and a fixed time method (25 s after injection started) in the r-VIBE-KWIC group. In the c-VIBE group, the signal in the ascending aorta was monitored, and the MRI was manually started 6 s after the contrast agent arrived at the ascending aorta. In the r-VIBE-KWIC group, we used the KWIC view-sharing technique, with arterial phase images yielding eight sub-frame images per one full-frame image. Eight interleaved subsets of projection views were acquired sequentially to form a full-frame set composed of 168–248 radial projection views (21–31 projection views per interleaved subset). In this manner, the volumetric set of contiguous axial images in r-VIBE-KWIC was divided into two subgroups, a dataset of full-frame images (r-VIBE$_{full}$) and a dataset of sub-frame images (r-VIBE$_{sub}$; temporal resolution, 2.5–3 s). The r-VIBE$_{sub}$ was available in all cases. Because of technical issues, the r-VIBE$_{full}$ was available in only 43 of 53 cases. Portal venous phase and hepatic venous phase images were not analysed in this study.

MRI analysis

Images in three groups (c-VIBE, r-VIBE$_{full}$, and r-VIBE$_{sub}$) were assessed based on four factors: degree of contrast enhancement in the aorta, scan timing, artefacts and the visualisation of arterial branches. We considered the degree of contrast enhancement in the aorta to be one of the index factors for detecting hypervascular lesions because a higher concentration of contrast material is more effective in

detecting hypervascular HCCs [21, 22]. All MR images were analysed with a commercial software package (EV Insite; PSP Corporation, Tokyo, Japan).

Quantitative assessment

To evaluate contrast enhancement, round regions of interest (ROIs) were placed on the abdominal aorta at the level of the celiac artery. The size of the ROIs was maximised without including extra-aortic structures. The signal intensity (SI) within the ROIs on precontrast and arterial phase images was measured by two experienced abdominal radiologists (Y.F. and A.O.). Because our protocol in the c-VIBE group included a parallel imaging method and was ineligible for signal-to-noise ratio (SNR) analysis, we calculated the contrast-enhancement ratio (CER) using the following equation:

$$CER = (SI_{enhanced} - SI_{unenhanced})/SI_{unenhanced}.$$

The mean SI of two values measured by two radiologists was used for calculation of the CER. In the r-VIBE$_{sub}$ group, the highest CER value among the eight sub-frame images was selected as the arterial phase SI (Fig. 1). We compared CERs among the three groups.

Qualitative assessment

To evaluate the timing of arterial phase DCE-MR images, two experienced abdominal radiologists (Y.F. and A.O.) independently defined the optimal timing by reference to previous reports as follows [23, 24]: an image on which (1) the hepatic artery (HA) was markedly enhanced, (2) the portal vein (PV) was inhomogeneously enhanced with laminar flow, (3) the hepatic vein (HV) was not enhanced, (4) the hepatic parenchyma was slightly enhanced. They recorded a 'markedly early arterial phase' when there was HA enhancement without PV, hepatic parenchymal or HV enhancement. They recorded an 'early arterial phase' when there was HA enhancement and minimal PV enhancement, but no hepatic parenchymal or HV enhancement. A 'late arterial phase' was defined by HA, PV (without laminar flow), hepatic parenchymal and faint HV enhancement. A 'markedly late arterial phase' was recorded when there was obvious HV enhancement. Based on this definition, the two readers also assessed the MRI timing using a three-point scale (3, optimal; 2, suboptimal; 1, unacceptable). In the r-VIBE$_{sub}$ group, each of the eight sub-frame images was assessed and the one with the highest score was selected for analysis.

To evaluate the quality of the images, the two readers assessed the degree of artefacts using a five-point scale (5, no artefact, diagnostic; 4, faint, diagnostic; 3, moderate, diagnostic; 2, intermediate, non-diagnostic; 1, strong, non-diagnostic) based on the visualisation of intrahepatic vessels and the homogeneity of the hepatic parenchyma (Fig. 2). In
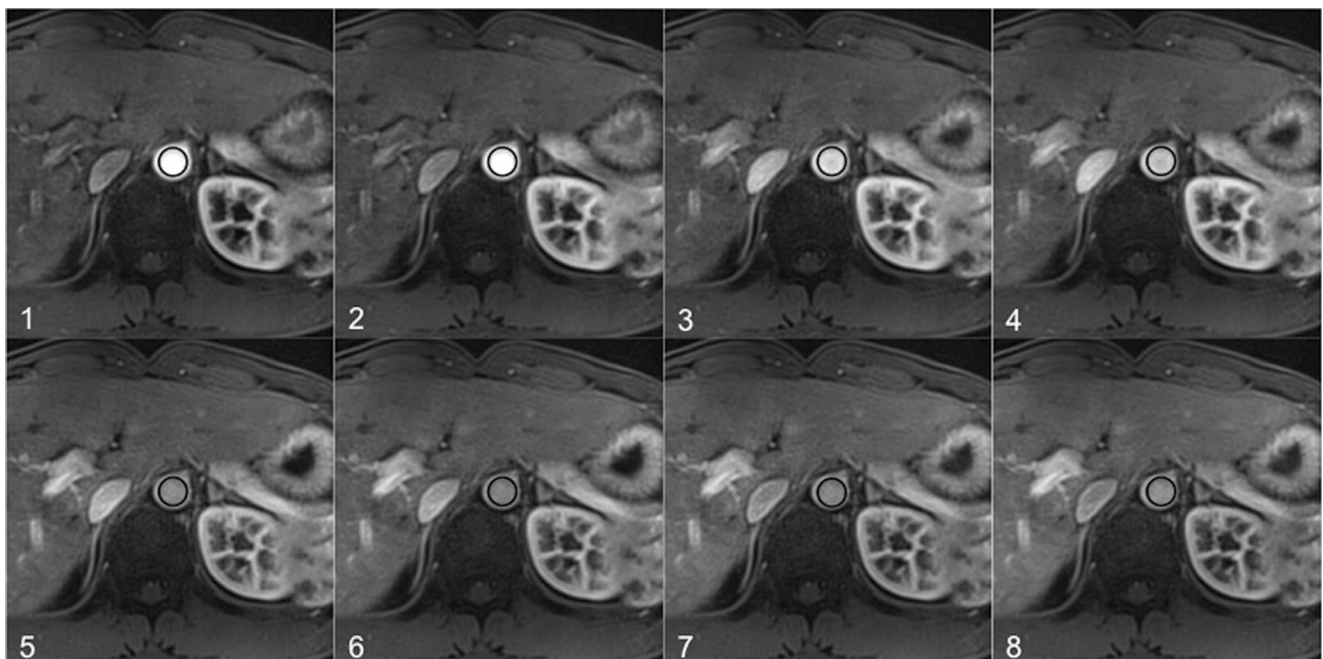

Fig. 1 A 41-year-old man with chronic liver disease. Arterial phase images of r-VIBE$_{sub}$ comprised eight sub-frame images. A region of interest is positioned on the aorta in all sub-frame images. The highest signal intensity (SI) of the aorta is selected for quantitative assessment. The SI on the first sub-frame image is selected in this case
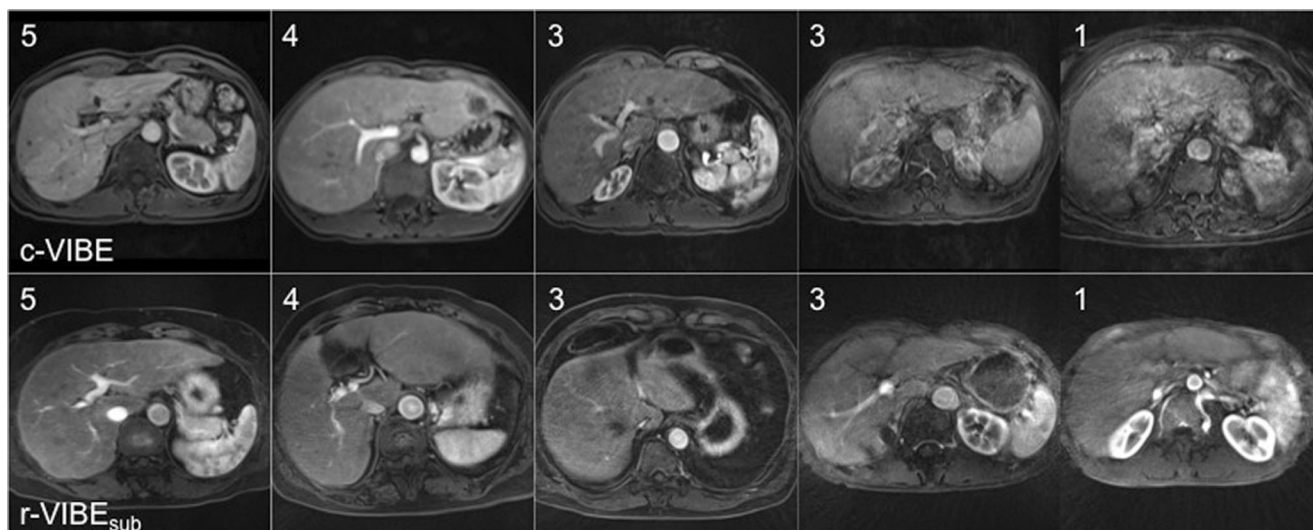
Fig. 2 Sample images for assessment of artefact. Images of c-VIBE are shown in the *upper row* and images of r-VIBE$_{sub}$ are in the *lower row. Leftmost* images in each row are scored 5 (no artefact, diagnostic) and *rightmost* images are scored 1 (strong artefact, non-diagnostic); *c-VIBE* Cartesian volumetric imaging breath-hold examination, *r-VIBE$_{sub}$* radial volumetric imaging breath-hold examination with k-space weighted image contrast reconstruction (sub-frame)

the r-VIBE$_{sub}$ group, a selected series of images acquired at the optimal time point was assessed.

Visualisation of hepatic arterial branches, such as common hepatic artery (CHA), right hepatic artery (RHA) and left hepatic artery (LHA), was also assessed by a five-point scale (5, very good, diagnostic; 4, good, diagnostic; 3, fair, diagnostic; 2, poor, non-diagnostic; 1, non-detectable). In r-VIBE$_{sub}$ group, a selected series of images acquired at the optimal time point was also selected for analysis. Values were given as the mean and range.

Statistical analysis

The Kruskal-Wallis test and Dunn's multiple comparison test were used to compare the values of each factor in the three groups. All statistical tests were two-tailed, and differences with $P<0.05$ were regarded as statistically significant. Kappa statistics were calculated to evaluate inter-reader agreement. A kappa value of 0.20 or less indicated poor agreement; 0.21–0.40, fair agreement; 0.41–0.60, moderate agreement; 0.61–0.80, good agreement; 0.81–1.00, excellent agreement. The statistical analysis was performed using software (Prism, version 5; GraphPad Software, La Jolla CA, USA and Microsoft Excel 2008; Microsoft, Redmond WA, USA).

Results

The mean CER for c-VIBE, r-VIBE$_{full}$ and r-VIBE$_{sub}$ was 3.2 (range, 1.3–6.4), 4.3 (range, 2.3–8.7) and 6.5 (range, 2.7–12.7), respectively. The mean CER for r-VIBE$_{sub}$ was significantly higher than that for c-VIBE or r-VIBE$_{full}$ ($P<0.0001$), and the mean CER for r-VIBE$_{full}$ was significantly higher than that for c-VIBE ($P<0.0001$) (Fig. 3).

The mean score of MRI timing, artefact severity and visualisation in the three groups by the two readers is shown in Table 3. The mean timing score of r-VIBE$_{sub}$ was significantly higher than that of c-VIBE and r-VIBE$_{full}$ ($P<0.05$) (Table 3). Kappa values of timing were high (good agreement) in the r-VIBE$_{sub}$ group. Readers 1 and 2 gave score 3 (optimal) in 39 (74 %) and 33 of 53 (62 %) patients in the c-VIBE group, 31 (72 %) and 29 of 43 (67 %) patients in the r-VIBE$_{full}$ group and 51 (96 %) and 49 of 53 (92 %) patients in
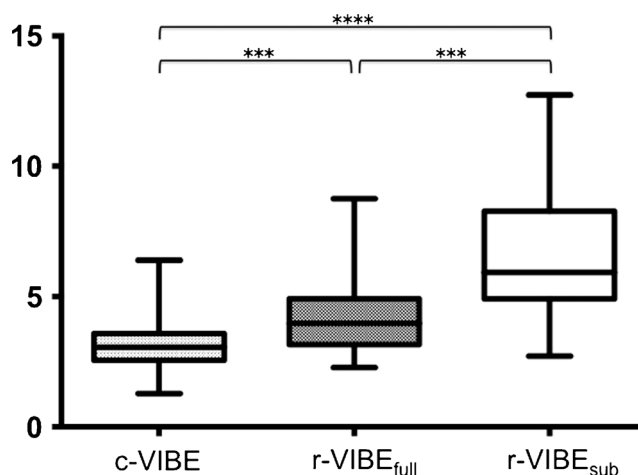

Fig. 3 Contrast-enhancement ratios of the three groups; *c-VIBE* Cartesian volumetric imaging breath-hold examination; *r-VIBE$_{full}$* radial volumetric imaging breath-hold examination with k-space weighted image contrast reconstruction (KWIC) (full-frame); *r-VIBE$_{sub}$* r-VIBE with KWIC (sub-frame); *** $P<0.0001$; **** $P<0.00001$

Table 3 Mean scores of each factor

Factor	Reader 1 Mean	Range		Reader 2 Mean	Range		Kappa value
Scan timing							
c-VIBE	2.6	1–3		2.5	1–3		0.343
r-VIBE$_{full}$	2.7	1–3	** *	2.6	1–3	** *	0.631
r-VIBE$_{sub}$	2.9	1–3		2.9	1–3		0.654
Artefact							
c-VIBE	3.2	1–5		3.2	1–5	**	0.944[a]
r-VIBE$_{full}$	4.0	2–5	** ****	3.8	2–5	*	0.788[a]
r-VIBE$_{sub}$	3.7	1–5		3.7	1–5		0.847[a]
Visualisation of HA							
CHA							
c-VIBE	3.3	2–5		3.0	1–5		0.547[a]
r-VIBE$_{full}$	3.6	2–5		3.5	1–5	**	0.726[a]
r-VIBE$_{sub}$	3.6	1–5		3.6	1–5		0.879[a]
RHA							
c-VIBE	3.1	1–5		2.8	1–5		0.570[a]
r-VIBE$_{full}$	3.9	1–5	*** ***	3.6	1–5	* **	0.655[a]
r-VIBE$_{sub}$	3.8	2–5		3.7	1–5		0.648[a]
LHA[g]							
c-VIBE	2.9	1–5		2.6	1–5		0.415[a]
r-VIBE$_{full}$	3.6	1–5	** ***	3.5	1–5	**** ***	0.640[a]
r-VIBE$_{sub}$	3.6	1–5		3.5	1–5		0.449[a]

c-VIBE Cartesian volumetric imaging breath-hold examination, *r-VIBE$_{full}$* radial VIBE with k-space weighted image contrast (full-frame), *c-VIBE* radial VIBE with k-space weighted image contrast (sub-frame); *HA* hepatic artery, *CHA* common hepatic artery, *RHA* right hepatic artery, *LHA* left hepatic artery

* $P<0.05$, ** $P<0.01$, *** $P<0.001$, **** $P<0.0001$

[a] Kappa values were calculated with the scores 1–2 considered non-diagnostic and 3–5 diagnostic

the r-VIBE$_{sub}$ group, respectively. In the r-VIBE$_{sub}$ group, improvement in the score was seen in all the cases (reader 1 and 2) that were scored 1 or 2 in r-VIBE$_{full}$ group (Fig. 4).

The mean artefact score of c-VIBE was significantly lower than that of r-VIBE$_{full}$ and r-VIBE$_{sub}$ ($P<0.05$). When the scores 1–2 were considered non-diagnostic and 3–5 diagnostic, kappa values in all groups were 0.788–0.944 (good or excellent agreement).

There was no significant difference in the mean score of CHA visualisation among the three groups except for between c-VIBE and r-VIBE$_{sub}$ according to reader 2. The mean score of RHA visualisation in c-VIBE was significantly lower than that in r-VIBE$_{full}$ and r-VIBE$_{sub}$ by the two readers ($P<0.05$) (Fig. 5). The mean score of LHA visualisation in c-VIBE was also significantly lower than that in r-VIBE$_{full}$ and r-VIBE$_{sub}$ ($P<0.01$). Again, with a score of 1–2 considered non-diagnostic and 3–5 diagnostic, agreement between the two readers was varied, but there were no instances of poor agreement.

Discussion

In this study, the CER in r-VIBE$_{sub}$ was significantly higher than that in c-VIBE and r-VIBE$_{full}$. We attribute this finding to differences in temporal resolution. When the total acquisition time of DCE-MRI is 20 s, the sampling time for filling up a low-frequency region in k-space is approximately 10 s with c-VIBE. In this period, SI in the aorta changes rapidly. Therefore, the SI of the aorta during the arterial phase is dynamically averaged. The higher temporal resolution of the r-VIBE$_{sub}$ affords more accurate measurement of peak and dynamic changes in SI (Fig. 6). The CER of r-VIBE$_{full}$ was higher than that of c-VIBE. In this study,
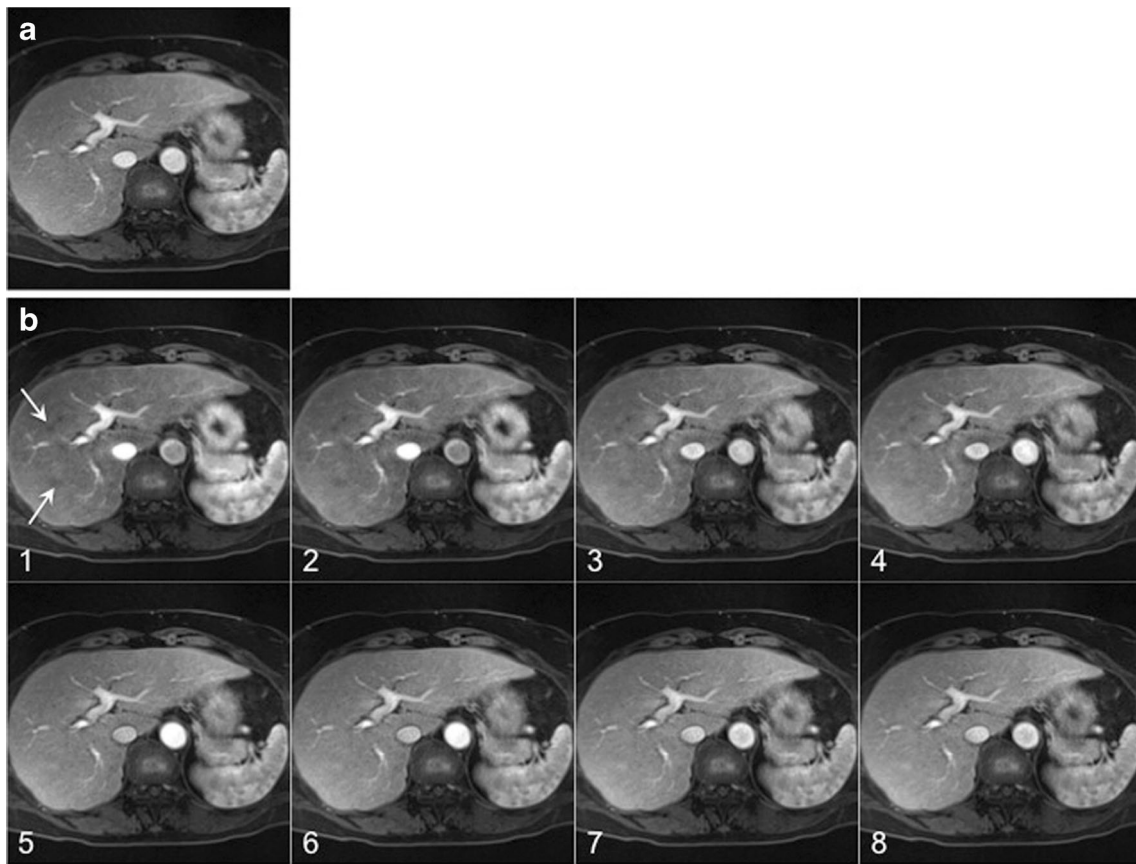
Fig. 4 Dynamic contrast-enhanced MRI using r-VIBE-KWIC in a 62-year-old-woman with chronic liver disease. On a full-frame image (**a**), laminar flow in the portal vein is seen, but the liver parenchyma is well enhanced and hepatic veins are unclear. This image was scored 2 by both readers. Among sub-frame images (**b**), the first sub-frame image was selected and scored 3 (optimal) by both readers because of laminar flow in the portal vein, slightly enhanced liver parenchyma, and unenhanced hepatic vein (*small white arrows*)

there were some differences between two groups involving parallel imaging, voxel size and the use of bolus tracking. In c-VIBE, we used a parallel imaging technique that tended to lower the SNR. The voxel size of c-VIBE (6.79 ± 0.64 mm^3) was significantly smaller than that of r-VIBE$_{full}$ (10.20 ± 1.80 mm^3) ($P<0.001$). The smaller voxel size in c-VIBE also tended to lower SNR. In c-VIBE, dynamic averaging of the bolus involved a risk of data sampling to start slightly before or slightly after the optimum intensity was achieved.

One of the interesting results in this study is that sub-frame images of r-VIBE-KWIC (r-VIBE$_{sub}$) were obtained at optimal timing more frequently than full-frame images. Namely, the high temporal resolution of r-VIBE$_{sub}$ provided optimal timing for arterial phase DCE-MRI, and high contrast enhancement. Optimal timing is one of the keys to accurate
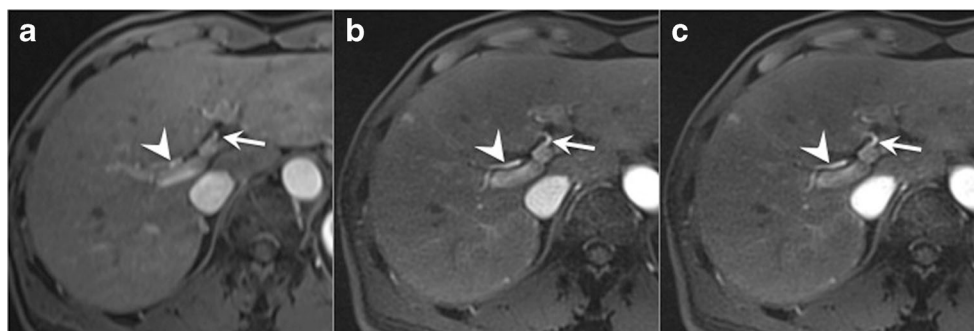

Fig. 5 Dynamic contrast-enhanced MRI using c-VIBE and r-VIBE-KWIC (4 years after c-VIBE) in a 66-year-old man with liver cirrhosis. **a** On the arterial phase of the c-VIBE image, the right (*white arrowhead*) and left hepatic artery (*white arrow*) can be detected. **b** On the arterial phase of the r-VIBE$_{full}$ image, the right (*white arrowhead*) and left (*white arrow*) hepatic artery are clearly seen. **c** On the arterial phase of the r-VIBE$_{sub}$ image (fourth sub-frame), the right (*white arrowhead*) and left (*white arrow*) hepatic artery are also clearly seen
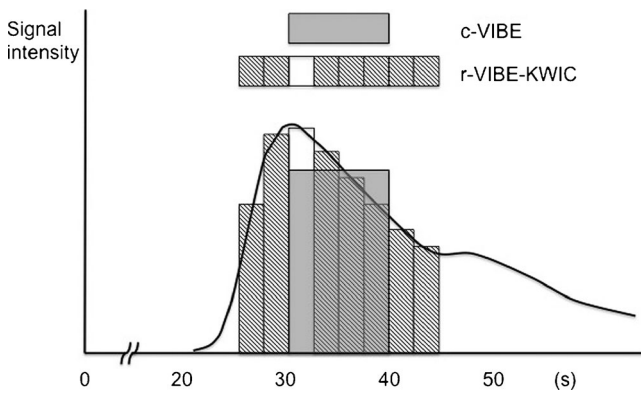
Fig. 6 Schematic image of the relation between time-intensity curve of the aorta and scan time. On c-VIBE, the sampling time of low-frequency region in k-space is approximately 10 s. The signal intensity of the aorta, though it varies markedly throughout the sampling time (*grey bar*), is averaged. The sampling time of r-VIBE with k-space weighted image contrast reconstruction (r-VIBE-KWIC) is approximately 20 s, but divided into eight sub-frames, each of whose temporal resolution is approximately 2.5 s (*diagonal bars*). The real peak signal intensity of the aorta is reflected in the sub-frame image (*white bar*) because of its high temporal resolution

lesion assessment. Previous studies have reported the value of multiple arterial phases for detection and characterisation of HCC [25, 26]. Lesion characterisation is outside the scope of this study; however, we show preliminary findings in the haemodynamics of HCC, which is commonly hypervascular. In Fig. 7, r-VIBE$_{sub}$ displays a more prominent early tumour stain compared with r-VIBE$_{full}$. Corona enhancement, one of the characteristic findings of HCC on CTHA [18], is also seen. However, improved haemodynamic evaluation was not validated in this study.

DCE-MRI of the abdomen is usually performed with breath-holding. There is an unavoidable trade-off between image quality and acquisition time (temporal resolution). The limit of breath-holding time for patients may be approximately 20 s, and not all patients can always achieve this task. This problem results in motion artefact in DCE-MRI with Cartesian view ordering technique (c-VIBE in this study). Radial view ordering technique has the advantage of overcoming motion artefact without degrading the image quality, because the central k-space region is repetitively sampled [27]. DCE-MRI with Cartesian view ordering technique has another
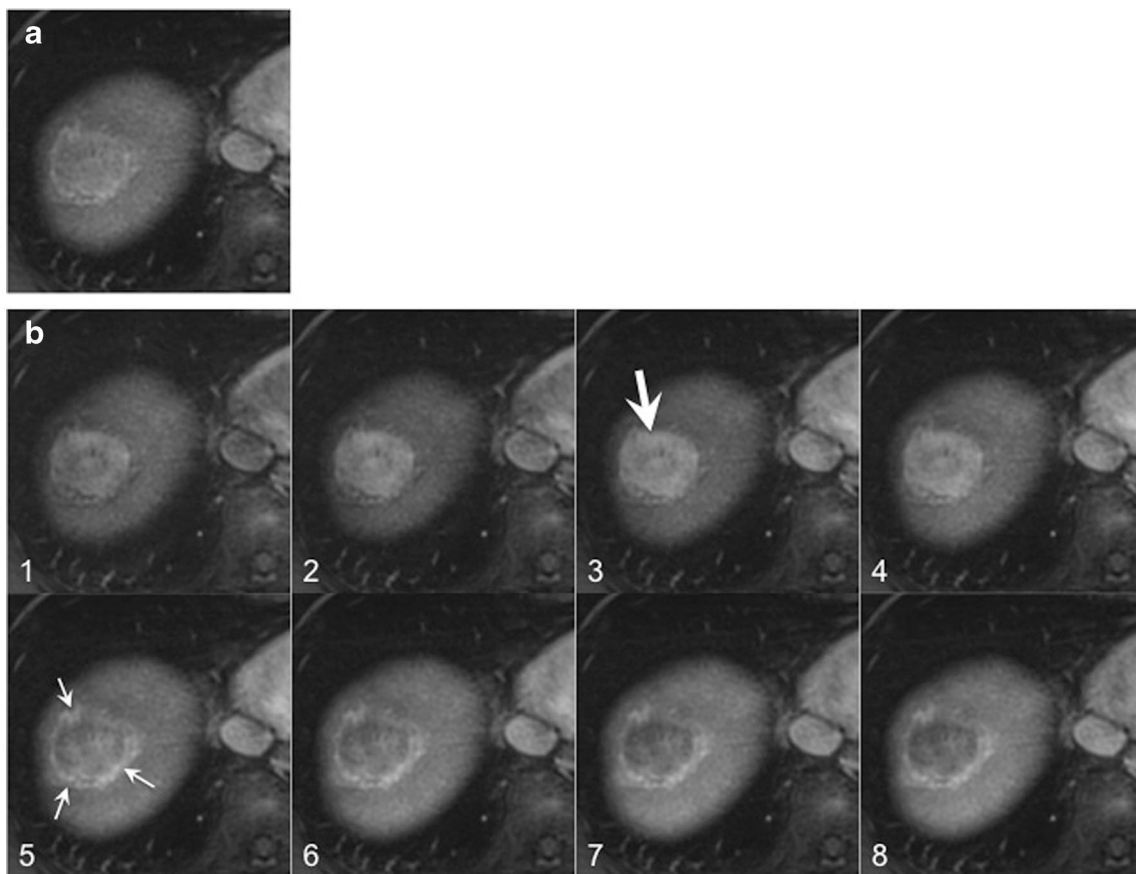

Fig. 7 An 81-year-old man with hepatocellular carcinoma (HCC) underwent dynamic contrast-enhanced MRI using r-VIBE with k-space weighted image contrast reconstruction (r-VIBE-KWIC). **a** On the r-VIBE-KWIC (full-frame image, r-VIBE$_{full}$) arterial phase image, a hypervascular HCC is seen. **b** On r-VIBE-KWIC arterial phase images (eight sub-frame images, r-VIBE$_{sub}$), enhancement of the HCC is most prominent in the third sub-frame image (*white arrow*) compared with the r-VIBE$_{full}$ image. Washout of the tumour and corona enhancement (*small white arrows*) are seen on the 5th-8th sub-frame images

problem of ringing artefact that degrades the quality of MR images. It is more prominent on DCE-MR images using GD-EOB-DTPA than Gd-DTPA because the time-intensity curve of the former has a single peak (short peak) pattern and the latter has a double peak (long peak) pattern [10]; i.e. sampled data of the former includes greater changes in the signal than the later. Though r-VIBE-KWIC images are theoretically less susceptible to image problems such as truncation and motion artefact, there is a characteristic artefact, the so-called 'streaking artefact', due to undersampling and/or susceptibility-related effect [14]. Though our qualitative assessment of artefact includes some of the above factors, motion and truncation artefact affected c-VIBE images and streaking artefact affected r-VIBE-KWIC images. In this study, the mean scores for artefacts in r-VIBE-KWIC (both r-VIBE$_{full}$ and r-VIBE$_{sub}$) were higher than those for c-VIBE. Our results suggest that truncation and motion artefact played a much more prominent role in degradation of image quality than streaking artefact. In addition, streaking artefact seems to be a minor problem because it can be reduced by the use of an iterative method for improving image quality in the arterial phase of DCE-MRI [28].

Visualisation of the RHA and LHA with r-VIBE$_{full}$ and r-VIBE$_{sub}$ was better than with c-VIBE. This result also suggests that r-VIBE-KWIC images are of higher quality than c-VIBE images. However, there was no significant difference in CHA visualisation among the three groups according to reader 1, and between c-VIBE and r-VIBE$_{full}$ according to reader 2. The CHA normally runs close to the PV. Hence, contrast between the CHA and PV, and good spatial resolution in the z-axis, are essential for visualisation. In this point, our results were acceptable because the slice thickness of r-VIBE-KWIC was slightly thicker than that of c-VIBE.

Another interesting result in our study is that the mean score of all factors in r-VIBE$_{sub}$ was not significantly lower than that in r-VIBE$_{full}$. In r-VIBE$_{sub}$, the number of the projection views in the central k-space region was one-eighth that of r-VIBE$_{full}$ because we used eight sub-frame images. A small number of projection views causes streaking artefact, i.e. deteriorates image quality [14, 28]. However, the image quality of r-VIBE$_{sub}$ compared favourably with that of r-VIBE$_{full}$. This result also suggests that streaking artefact is a minor problem and r-VIBE$_{sub}$, having both less artefact and higher temporal resolution, is the most useful for detection and characterisation of liver lesions.

Limitations of our study are, first, varied sequence parameters for the two sequences. However, we believe that it was minor because each sequence was optimised for clinical examination. However, the voxel size of c-VIBE was significantly smaller than that of r-VIBE-KWIC ($P<0.001$); i.e. the resolution of c-VIBE was higher than that of r-VIBE-KWIC. Our results suggest that the image quality of r-VIBE was higher than that of c-VIBE regardless of the lower resolution

of r-VIBE-KWIC. However, we should note that the smaller voxel size of c-VIBE than that of r-VIBE-KWIC in this study introduces bias because a small voxel size is considered a disadvantage for high SNR images. Second, there were some variations in the case characteristics in each group, though there was no statistically significant demographic difference between the two groups. Third, the delay time of the arterial phase in the r-VIBE$_{full}$ and r-VIBE$_{sub}$ groups was fixed. Kagawa et al. [29] reported that the time of peak aortic enhancement was 21.0 ± 5.9 s and the time of peak HCC enhancement was 29.9 ± 4.6 s after injection of Gd-EOB-DTPA (at a rate of 2 ml/s). Thus, the peak CER of the aorta in r-VIBE$_{full}$ and r-VIBE$_{sub}$ group might be underestimated, though the timing of the arterial phase was optimal. Bolus tracking technique may improve this issue.

In conclusion, r-VIBE-KWIC (r-VIBE$_{full}$ and r-VIBE$_{sub}$) provided higher image quality than c-VIBE in our setup, and the r-VIBE$_{sub}$ was characterised by high temporal resolution without degradation of the images on arterial phase DCE-MRI.

References

1. Schuhmann-Giampieri G, Schmitt-Willich H, Press WR, Negishi C, Weinmann HJ, Speck U (1992) Preclinical evaluation of Gd-EOB-DTPA as a contrast agent in MR imaging of the hepatobiliary system. Radiology 183:59–64
2. Reimer P, Rummeny EJ, Shamsi K et al (1996) Phase II clinical evaluation of Gd-EOB-DTPA: dose, safety aspects, and pulse sequence. Radiology 199:177–183
3. Huppertz A, Balzer T, Blakeborough A et al (2004) Improved detection of focal liver lesions at MR imaging: multicenter comparison of gadoxetic acid-enhanced MR images with intraoperative findings. Radiology 230:266–275
4. Bluemke DA, Sahani D, Amendola M et al (2005) Efficacy and safety of MR imaging with liver-specific contrast agent: U.S. multicenter phase III study. Radiology 237:89–98
5. Hammerstingl R, Huppertz A, Breuer J et al (2008) Diagnostic efficacy of gadoxetic acid (Primovist)-enhanced MRI and spiral CT for a therapeutic strategy: comparison with intraoperative and histopathologic findings in focal liver lesions. Eur Radiol 18:457–467
6. Petersein J, Spinazzi A, Giovagnoni A et al (2000) Focal liver lesions: evaluation of the efficacy of gadobenate dimeglumine in MR imaging—a multicenter phase III clinical study. Radiology 215:727–736

7. Brismar TB, Dahlstrom N, Edsborg N, Persson A, Smedby O, Albiin N (2009) Liver vessel enhancement by Gd-BOPTA and Gd-EOB-DTPA: a comparison in healthy volunteers. Acta Radiol 50:709–715

8. Tamada T, Ito K, Sone T et al (2009) Dynamic contrast-enhanced magnetic resonance imaging of abdominal solid organ and major vessel: comparison of enhancement effect between Gd-EOB-DTPA and Gd-DTPA. J Magn Reson Imaging 29:636–640

9. Kuhn JP, Hegenscheid K, Siegmund W, Froehlich CP, Hosten N, Puls R (2009) Normal dynamic MRI enhancement patterns of the upper abdominal organs: gadoxetic acid compared with gadobutrol. AJR Am J Roentgenol 193:1318–1323

10. Fujinaga Y, Ueda H, Kitou Y, Tsukahara Y, Sugiyama Y, Kadoya M (2012) Time-intensity curve in the abdominal aorta on dynamic contrast-enhanced MRI with high temporal and spatial resolution: Gd-EOB-DTPA versus Gd-DTPA in vivo. Jpn J Radiol 31:166–171

11. Tanimoto A, Lee JM, Murakami T, Huppertz A, Kudo M, Grazioli L (2009) Consensus report of the 2nd International Forum for Liver MRI. Eur Radiol 19:S975–S989

12. Svensson J, Petersson JS, Stahlberg F, Larsson EM, Leander P, Olsson LE (1999) Image artifacts due to a time-varying contrast medium concentration in 3D contrast-enhanced MRA. J Magn Reson Imaging 10:919–928

13. Vigen KK, Peters DC, Grist TM, Block WF, Mistretta CA (2000) Undersampled projection-reconstruction imaging for time-resolved contrast-enhanced imaging. Magn Reson Med 43:170–176

14. Song HK, Dougherty L (2004) Dynamic MRI with projection reconstruction and KWIC processing for simultaneous high spatial and temporal resolution. Magn Reson Med 52:815–824

15. Kim KW, Lee JM, Jeon YS et al (2012) Free-breathing dynamic contrast-enhanced MRI of the abdomen and chest using a radial gradient echo sequence with K-space weighted image contrast (KWIC). Eur Radiol 23:1352–1360

16. Kim JH, Lee JM, Park JH et al (2013) Solid pancreatic lesions: characterization by using timing bolus dynamic contrast-enhanced MR imaging assessment—a preliminary study. Radiology 266:185–196

17. Brodsky EK, Bultman EM, Johnson KM et al (2013) High-spatial and high-temporal resolution dynamic contrast-enhanced perfusion imaging of the liver with time-resolved three-dimensional radial MRI. Magn Reson Med. doi:10.1002/mrm.24727

18. Ueda K, Matsui O, Kawamori Y et al (1998) Hypervascular hepatocellular carcinoma: evaluation of hemodynamics with dynamic CT during hepatic arteriography. Radiology 206:161–166

19. Miyayama S, Matsui O, Ueda K et al (2000) Hemodynamics of small hepatic focal nodular hyperplasia: evaluation with single-level dynamic CT during hepatic arteriography. AJR Am J Roentgenol 174:1567–1569

20. Griswold MA, Jakob PM, Heidemann RM et al (2002) Generalized autocalibrating partially parallel acquisitions (GRAPPA). Magn Reson Med 47:1202–1210

21. Yagyu Y, Awai K, Inoue M et al (2005) MDCT of hypervascular hepatocellular carcinomas: a prospective study using contrast materials with different iodine concentrations. AJR Am J Roentgenol 184:1535–1540

22. Sofue K, Tsurusaki M, Kawasaki R, Fujii M, Sugimura K (2011) Evaluation of hypervascular hepatocellular carcinoma in cirrhotic liver: comparison of different concentrations of contrast material with multi-detector row helical CT–a prospective randomized study. Eur J Radiol 80:e237–e242

23. Chung SH, Kim MJ, Choi JY, Hong HS (2010) Comparison of two different injection rates of gadoxetic acid for arterial phase MRI of the liver. J Magn Reson Imaging 31:365–372

24. Haradome H, Grazioli L, Tsunoo M et al (2010) Can MR fluoroscopic triggering technique and slow rate injection provide appropriate arterial phase images with reducing artifacts on gadoxetic acid-DTPA (Gd-EOB-DTPA)-enhanced hepatic MR imaging? J Magn Reson Imaging 32:334–340

25. Ito K, Fujita T, Shimizu A et al (2004) Multiarterial phase dynamic MRI of small early enhancing hepatic lesions in cirrhosis or chronic hepatitis: differentiating between hypervascular hepatocellular carcinomas and pseudolesions. AJR Am J Roentgenol 183:699–705

26. Mori K, Yoshioka H, Takahashi N et al (2005) Triple arterial phase dynamic MRI with sensitivity encoding for hypervascular hepatocellular carcinoma: comparison of the diagnostic accuracy among the early, middle, late, and whole triple arterial phase imaging. AJR Am J Roentgenol 184:63–69

27. Glover GH, Noll DC (1993) Consistent projection reconstruction (CPR) techniques for MRI. Magn Reson Med 29:345–351

28. Block KT, Uecker M, Frahm J (2007) Undersampled radial MRI with multiple coils. Iterative image reconstruction using a total variation constraint. Magn Reson Med 57:1086–1098

29. Kagawa Y, Okada M, Kumano S et al (2011) Optimal scanning protocol of arterial dominant phase for hypervascular hepatocellular carcinoma with gadolinium-ethoxybenzyl-diethylenetriamine pentaacetic acid-enhanced MR. J Magn Reson Imaging 33:864–872